Photoemission study of the growth, desorption, Schottky-barrier formation, and atomic structure of Pb on Si(111)

J. A. Carlisle, T. Miller, and T.-C. Chiang
Department of Physics, University of Illinois at Urbana-Champaign, 1110 West Green Street, Urbana, Illinois 61801 and Materials Research Laboratory, University of Illinois at Urbana-Champaign, 104 South Goodwin Avenue, Urbana, Illinois 61801
(Received 25 September 1991)

We have utilized high-resolution synchrotron-radiation photoemission spectroscopy and high-energy electron diffraction to study the various reconstructed surfaces of Pb-covered Si(111). The Si 2*p* and Pb 5*d* core levels and valence bands are analyzed as a function of Pb coverage and annealing temperature. We confirm the room-temperature (RT) Stranski-Krastanov growth mode with the two-dimensional adlayer completed at ~ 1.3 monolayers. The formation of the Schottky barrier has been studied. We measure *n*-type barrier heights of 0.89 and 1.09 eV for the RT epitaxial phase and the $(\sqrt{3}\times\sqrt{3})R30°$ incommensurate phase, respectively. Possible mechanisms that may be responsible for the disagreement between barrier heights as measured by core-level photoemission and electrical techniques are discussed. We also report on the observation of surface-shifted core levels and surface states in the valence band for the $(\sqrt{3}\times\sqrt{3})R30°$ phases obtained by annealing to higher temperatures in the desorption regime. These results are used for an investigation of the structural models for these surface phases.

I. INTRODUCTION

For several years now, metal-semiconductor interfaces have received much attention owing to their great technological and fundamental interest. The ever increasing packing density of integrated circuits has made necessary an atomic-scale understanding of these systems. The fundamental mechanisms which determine Schottky-barrier formation in various systems remain a subject of active investigation. To this end, the study of nonreactive metal-semiconductor systems such as Pb on Si(111) is of basic interest. Pb adlayers on silicon and germanium substrates have been considered prototypical systems, since their phase diagrams show no stable silicides or germanides and the mutual solubilities are negligibly small at the Pb melting point.[1] Heslinga *et al.*,[2] using electrical measurements, reported that the Schottky barrier for a Pb overlayer on Si(111) depended strongly on the interface preparation procedure, implying that the barrier height is sensitive to the interfacial atomic structure. Their work led to a recent debate on a separate issue concerning the difference in Schottky-barrier heights as determined by electrical and photoemission techniques.[3,4] To explain this difference, Karlsson, Nyqvist, and Kanski emphasized that final-state effects might be significant due to metal-overlayer-induced core-hole screening, which should be accounted for in the use of core-level photoemission to determine Schottky-barrier heights.[5] They also cited the Pb/Si(111) system as a candidate for this effect. In this work, we examine these issues by presenting photoemission results for the Schottky-barrier height of Pb/Si(111) for two different overlayer structures. The barrier heights found for these two structures are compared with those reported by Heslinga *et al.*, and the differences are discussed in light of the various ideas discussed in the literature.

The various reconstructions exhibited by the Pb/Si(111) system have also been a subject of intensive research, yet there remains confusion in the literature over the number of stable phases and their corresponding coverages and atomic structure. An early study by Estrup and Morrison using low-energy electron-diffraction (LEED) proposed epitaxial growth of Pb on Si(111) at room temperature (RT), with the adlayer completed at $\frac{4}{3}$ ML.[6] Upon annealing at 300 and 400 °C briefly, they found two $(\sqrt{3}\times\sqrt{3})R30°$ reconstructions, with coverages of $\frac{4}{3}$ and $\frac{1}{3}$ ML, respectively. These results were confirmed and extended more recently by Saitoh *et al.*,[7] using low-energy ion scattering, and by Yaguchi, Baba, and Kinbara[8] using high-energy electron diffraction (HEED), who both found that Pb grows in the Stranski-Krastanov (SK) mode with the two-dimensional adlayer completed at ~ 1.3 ML. Then Le Lay and coworkers,[1,9–13] using a variety of techniques, proposed a quite different picture. They found the first adlayer to be completed at 1 ML, with the (7×7) LEED pattern gradually changing to a (1×1) periodicity. Their results also indicated three distinct phases with the same $(\sqrt{3}\times\sqrt{3})R30°$ periodicity but at coverages of $\frac{1}{3}$, $\frac{2}{3}$, and 1 ML. Grey *et al.*,[14] using surface x-ray diffraction (SXRD), found the RT-grown two-dimensional adlayer to be a commensurate 8×8 close-packed configuration per (7×7) unit cell, which indicated a completion coverage of $\frac{64}{49}=1.31$ ML. They also reported that, after annealing this RT-prepared layer to ~ 200 °C, the surface structure became an incommensurate close-packed layer, rotated by 30° with respect to the RT phase. Recently, Ganz *et al.*[15] performed a scanning tunneling microscopy (STM) study of this system and found a low-coverage $(\sqrt{3}\times\sqrt{3})R30°$ phase, which has both Si and

Pb adatoms in a T_4 geometry with an ideal Pb coverage of $\frac{1}{6}$ ML. The T_4 geometry has also been suggested based on recent tensor LEED calculations.[16] In addition to the above-mentioned irreversible changes in reconstruction induced by thermal annealing and desorption, Pb monolayers on Si(111) and Ge(111) show a reversible phase transition which has been attributed, in the case of Ge, to a two-dimensional melting transition.[1,17]

In an effort to clarify some of the unresolved issues just mentioned and to gain a better understanding of the surface structure, we have undertaken a systematic study of the RT growth and subsequent annealing and desorption of Pb on Si(111) surfaces using HEED and photoemission. Although some photoemission data have been discussed in previous work,[1,10,11,18,19] a thorough and complete study is lacking. Our measurements confirm the SK growth mode for RT adsorption, with the first adlayer completed at ~ 1.3 ML. Our annealing and desorption data indicate the existence of three $(\sqrt{3}\times\sqrt{3})R30°$ phases, labeled α, β, and γ, with ideal Pb coverages of 1.3, $\frac{1}{3}$ and $\frac{1}{6}$ ML, respectively. The β and γ phases display surface-shifted core levels and surface states in the valence band which are consistent with a simple T_4 adatom geometry. These results are used for an investigation of the possible structures of these reconstructions.

II. EXPERIMENTAL DETAILS

The photoemission experiments were performed on the 1-GeV storage ring Aladdin at the Synchrotron Radiation Center of the University of Wisconsin-Madison. Synchrotron radiation was dispersed using an extended-range grating monochrometer. A large hemispherical analyzer was employed to detect electrons emitted from the sample in an angle-integrating mode. All binding energies were measured relative to the Fermi level, which was taken from a gold foil in electrical contact with the sample. The overall experimental resolution was between 100 and 170 meV, depending on the photon energy used. All spectra were taken with the sample at or near room temperature.

The Si(111) samples used were cut from n-type wafers into $13\times5\times0.15$ mm^3 rectangles, and mounted onto stainless-steel sample holders via tantalum clips. Preparation of a (7×7) reconstructed surface consisted of outgassing overnight at ~ 500 °C, followed by a 2-h cool down and then flashing to ~ 1250 °C for 7–10 sec. This procedure consistently yields very sharp HEED patterns as well as strongly pronounced surface-shifted core-level components and well-defined surface-state features in the valence band. High-purity (99.999%) Pb was evaporated from a tungsten crucible heated with a feedback-controlled electron beam. The deposition rate was measured using a quartz-crystal thickness monitor; the uncertainty in absolute coverage was less than $\pm 10\%$.[20] The coverage units used throughout this work are referred to the Si(111) unreconstructed substrate: 1 monolayer (ML) $= 7.83\times10^{14}$ atoms/cm^2 = one-half of a Si(111) double layer.

The core-level decomposition procedure used throughout this work is the same as has been used in numerous previous studies.[20–23] A nonlinear least-squares method was employed utilizing Voigt line shapes (convolution of a Gaussian and a Lorentzian) to represent each spin-orbit-split component. Each spectrum was assumed to consist of several such doublets, representing the bulk and surface-shifted contributions, on top of a smooth cubic polynomial to approximate the secondary-electron background.

III. RESULTS AND DISCUSSION

A. RT growth

Upon deposition of Pb onto a clean Si(111)-(7×7) surface, the HEED pattern gradually evolves into one with the same (7×7) periodicity, but with a higher background and a much altered intensity distribution. Only the $\frac{6}{7}$ and $\frac{8}{7}$ fractional-order spots remain visible. This result is in agreement with other HEED (Ref. 8) and LEED (Ref. 7) work, but is in disagreement with Le Lay *et al.*,[9] who observed a gradual vanishing of the $\frac{1}{7}$ order spots in the initial (7×7) pattern, leaving a (1×1) structure above 1-ML Pb coverage. There also exists a question as to the completion coverage of the RT phase; most groups assign $\sim\frac{4}{3}$ ML to the adlayer coverage, whereas Le Lay and co-workers have proposed a 1-ML completion coverage for the RT phase.

We have studied the modification of the Si $2p$ and Pb $5d$ core levels as a function of Pb coverage. In Fig. 1 we show the changes of the absolute Pb $5d$ intensity as well as the intensity ratio of the Pb $5d$ to Si $2p$ cores versus Pb

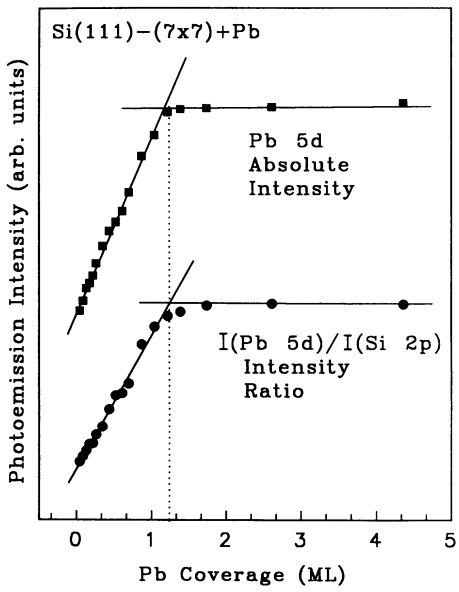

FIG. 1. The Pb $5d$ absolute intensity (upper curve) and the intensity ratio of Pb $5d$ to Si $2p$ cores (bottom curve) are plotted as a function of Pb coverage. The Si $2p$ intensities were acquired using bulk-sensitive data (i.e., with 110-eV photon energy). The vertical dotted line indicates a break in the linear progressions of both curves at 1.3-ML Pb coverage. The two curves are not to the same scale.

coverage. As is apparent upon inspection of Fig. 1, the RT growth follows the SK mode (formation of a two-dimensional adlayer followed by three-dimensional islands), with a clearly defined break in the linear progressions of both curves at about 1.3 ML. This is in very good agreement with the $\frac{64}{49}=1.31$ ML proposed by Grey *et al.*[14] in their SXRD work.

In Fig. 2, selected Si $2p$ core-level spectra obtained using either 110-eV photons (bulk sensitive) or 150-eV photons (surface sensitive) are shown. The surface-sensitive spectrum for the clean surface exhibits two surface-shifted components ($S1$ and $S2$) in addition to the bulk component ($S0$);[21–23] the decomposition of the spectrum into these components is indicated by the various curves. As increasing amounts of Pb are deposited on the surface, two things happen: (1) the line shape changes due to Pb-induced chemical shifts (see the surface-sensitive spectra) and (2) the bulk component shifts to lower binding energy due to band bending (see the bulk-sensitive spectra).

The surface-sensitive spectra in Fig. 2 show that the line sharpens for increasing Pb coverages. A detailed analysis involving fitting the spectra shows that the intensities of the surface components relative to the bulk component are gradually reduced to zero for increasing Pb coverages from 0 to 1.3 ML. The line shape remains unchanged for coverages beyond 1.3 ML. These results can be interpreted as follows. The deposited Pb saturates the dangling bonds on the Si(111)-(7×7) surface, and possibly induces modifications to the substrate (7×7) structure. As a result, the Si surface atoms sense a bulklike environment, and hence the surface shifts are suppressed. This suppression becomes complete at 1.3 ML, when the surface becomes fully covered with Pb. We note that the SXRD study of Grey *et al.*[14] found a slightly better fit of the observed experimental data for a model with a close-packed Pb overlayer on an unrelaxed stacking-faulted Si bilayer, but with no Si adatoms. This model shows that all Si surface atoms are covered by Pb and is consistent with our core-level results. One might wonder what happens to the Si adatoms on the original (7×7) surface during the Pb deposition. It is possible that these adatoms are moved by the Pb deposition to nearby step edges where they become incorporated into the neighboring terraces.

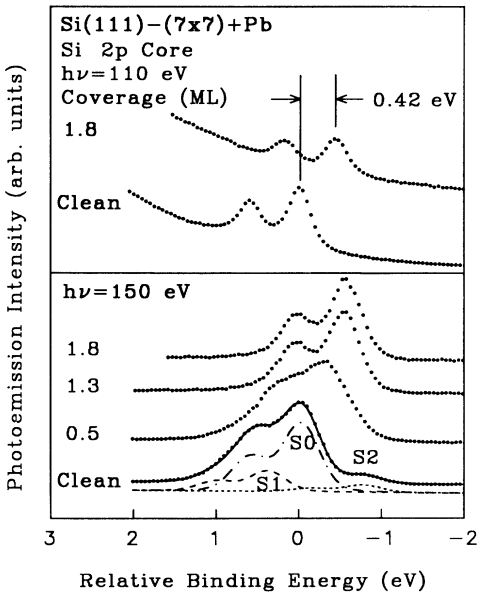

FIG. 2. Selected Si $2p$ spectra acquired at various Pb coverages, using either 110-eV photons (upper curves, bulk sensitive) or 150-eV photons (bottom curves, surface sensitive). The Pb coverage associated with each spectrum is shown on the left. The circles are data points and the line through them is the least-squares fit. The surface-shifted components $S1$ and $S2$ and the bulk component ($S0$) for the clean surface are indicated by the various curves under the spectrum. The 0.42-eV shift to lower binding energy, shown in the top spectra, shows the band bending induced by the deposition of 1.8 ML of Pb at RT.

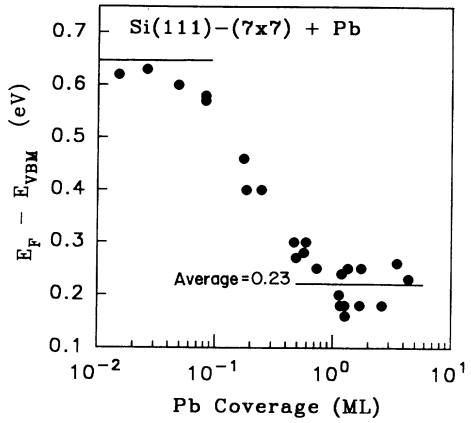

FIG. 3. The Fermi-level position, with respect to the valence-band maximum (VBM), is plotted as a function of the logarithm of the Pb coverage, in ML. The horizontal line at 0.65 eV above the VBM denotes the pinning position for the clean surface.

The band bending can be deduced from the line shifts in the bulk-sensitive spectra. For example, the two upper spectra in Fig. 2 show that the Si $2p$ core shifts by −0.42 eV for 1.8-ML Pb coverage relative to the clean surface. Since the pinning position of the Fermi level for the clean Si(111)-(7×7) surface is 0.65 eV above the valence-band maximum (VBM),[24] we can determine, from the core shifts, the Fermi-level movement within the Si band gap as a function of Pb coverage. The results are shown in Fig. 3. We determine an n-type Schottky-barrier height of 0.89 eV for the RT epitaxial phase. The data scatter in Fig. 3 indicates a precision of about ±0.03 eV. This measured Schottky-barrier height will be discussed below.

B. The α phase

The RT phase is metastable, and an irreversible phase transition occurs when the system is heated to 200–240 °C. After annealing, the RT epitaxial Pb (7×7) HEED pattern is converted into an "apparent" $(\sqrt{3}\times\sqrt{3})R30°$ one, where the $\frac{1}{3}$-order spots are considerably diffuse and elongated as compared to the bulk spots. The background is also reduced somewhat as com-

pared with the RT phase. Following the literature, we will denote this phase as the α phase ($R30°i$ is used by Grey *et al.*). Interestingly, one may obtain this phase by depositing greater than 1.3 ML onto samples held at even lower temperatures, in the 120°C–200°C range. Apparently, the condensation energy released by the excess Pb allows the system to overcome the transition barrier at a lower substrate temperature. The α phase has the same completion coverage (1.3 ML) as the RT phase. Any excess Pb on the surface remains in the form of highly three-dimensional Pb islands (SK growth mode). Although the HEED pattern looks like a diffuse $(\sqrt{3}\times\sqrt{3})R30°$, the SXRD studies by Grey *et al.*[14] have found this phase to in fact be an incommensurate close-packed Pb layer, with Pb $[1\bar{1}0]\|$Si $[1\bar{2}1]$, i.e., the Pb [10] axis is rotated 30° with respect to the Si [10] axis.

Annealing this α phase to about 280°C triggers a *reversible* phase transition to a (1×1) periodicity. A similar transition has been noted for the Pb on Ge(111) system, which has been attributed to a two-dimensional melting transition.[1,17]

In Fig. 4 we compare the Si 2*p* core-level spectra obtained for the RT and α phases. The RT-prepared sample had a Pb coverage of 1.8 ML, and the surface was an epitaxial Pb overlayer (1.3 ML) plus three-dimensional Pb islands (0.5 ML) covering a small fraction of the total surface area. The α phase was obtained by annealing the RT prepared sample at 240°C, and also had 0.5 ML of excess Pb in the form of three-dimensional islands. The top panel shows the bulk-sensitive spectra; a band-bending shift of 0.20 eV to lower binding energy is seen in going from the RT phase to the α phase. Combining this result with that for the RT phase discussed earlier, we deduce a Schottky-barrier height of 1.09 eV for the α phase. This result will be discussed below.

The surface-sensitive core-level spectra are shown in the lower panel of Fig. 4. To compare the line shapes in detail, the spectrum for the α phase (solid curve) has been moved by 0.20 eV to higher binding energy. This removes the band-bending shift, so the two line shapes are "aligned." The comparison shows a narrowing of the line shape as the RT phase is converted into the α phase, as revealed by the deepening of the valley between the spin-orbit split peaks. This means that small, unresolved near-surface shifts for the RT phase are suppressed by the transformation into the α phase. Since both phases have a close-packed Pb overlayer on the surface as determined by the SXRD work (the difference being a rotation of the overlayer by 30°), it is unlikely that Pb-induced chemical shifts are responsible for the line-shape change. We interpret this narrowing as the result of the reversal of the stacking fault by the annealing, with the underlying Si(111) substrate changing to a bulklike termination. The removal of the stacking fault yields a concomitant sharpening of the Si 2*p* core due to a reduction in the number of inequivalent sites for the Si atoms present in the first bilayer under the Pb. The removal of the stacking fault has also been suggested by the SXRD work. Thus, the best structural model for the α phase is a close-packed, 30°-rotated Pb monolayer on a bulk-truncated Si(111).

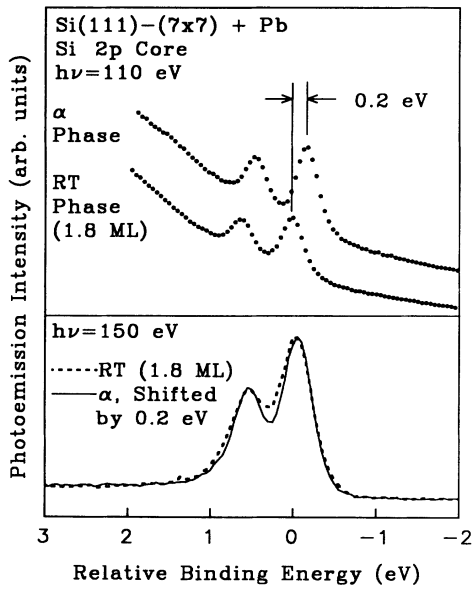

FIG. 4. Si 2*p* spectra obtained before and after annealing at 240°C for 1.8-ML Pb deposited on Si(111). The upper spectra (bulk sensitive) show the 0.20-eV band-bending shift induced through the conversion of the RT epitaxial phase into the incommensurate α phase. The bottom spectra are surface sensitive. For an easy comparison of the line shapes, the spectrum for the α phase has been shifted by 0.20 eV to compensate for the band-bending shift.

C. Schottky-barrier heights

Our measured values for the Schottky-barrier heights are 0.89 ± 0.03 and 1.09 ± 0.03 eV for the RT phase and the α phase, respectively. These are to be contrasted with $0.70\ \pm0.02$ eV and 0.93 ± 0.01 eV, respectively, based on capacitance-voltage measurements of Heslinga *et al.*[2] In these electrical measurements, the RT phase and the α phase were first prepared in ultrahigh vacuum and then a thick layer of Pb was laid over at room temperature. Clearly, there is a discrepancy between our values and those deduced from the electrical measurements. Our values are larger by about 0.18 eV in each case, yet the difference in barrier height between the two reconstructions, 0.20 eV in our case and 0.23 eV from the electrical measurements, is the same within the quoted experimental errors. As argued by Heslinga *et al.*, this barrier-height difference is associated with the structural difference between the two phases, and is a local effect specific to the interface. Therefore, it appears reasonable to expect the same barrier-height difference, even though the barrier heights themselves may be different due to the very different overlayer thicknesses involved in these two experiments. There are, however, complications to be discussed in the following.

Le Lay and co-workers have also performed barrier-height measurements for these two reconstructions based on the photoemission technique; their reported values are 0.87 and 0.97 eV for the RT phase and the α phase, re-

spectively.[1,3] They argued that the disagreement in barrier heights as deduced from electrical and photoemission data can be accounted for based solely on structural changes induced by the presence of a thick Pb overlayer on the reconstructed surfaces. Karlsson, Nyqvist, and Kanski, however, thought that the difference could be due to final-state screening effects in photoemission, and cautioned that extreme care should be exercised in using photoemission for barrier-height determination.[5] Thus, three issues need to be addressed. The first issue is why our values are different from those of Le Lay and co-workers. The second issue is whether or not the barrier heights deduced from photoemission and electrical measurements are supposed to be the same. The third issue concerns the possible dependence of the barrier height on the overlayer thickness. These are discussed in the following.

The difference between our results and those reported by Le Lay and co-workers might be due to sample differences. As mentioned earlier, some of their reported reconstructions and completion coverages are different from the results reported by most other authors. This led to our supposition; however, we have no means of verifying this point.

Concerning the second issue (photoemission versus electrical measurements), it has been pointed out by various authors that photoemission results are susceptible to errors due to subsurface core-level shifts.[5,25] Even for bulk-sensitive spectra, the core-level signal does not really come from the bulk, but represents a weighted average involving ~ 10 atomic layers. In this regard, we note that the calculation of Karlsson, Nyqvist, and Kanski[5] is not applicable in the present comparison. Their calculation is for a *semi-infinite* metal overlayer on a semiconductor surface. Their results show that final-state screening of the core hole in the near-surface region of the semiconductor by the metal overlayer can cause up to ~ 0.2-eV shift relative to the true bulk value, resulting in a corresponding error in the band bending. However, most photoemission measurements, including the present one, are limited to overlayers with a thickness of ~ 1 ML due to problems of signal strength associated with thicker overlayers. For these thin overlayers, the screening effect should be much less important. Furthermore, the overlayers are only weakly metallic. Our photoemission results from the valence bands, to be presented below, show that the density of states is quite small at the Fermi level for the RT and $(\sqrt{3}\times\sqrt{3})R30°$ phases. The screening effect of the Pb overlayer is probably on the same order as that would be expected for a Si overlayer on the Si substrate. Core holes near a surface will be less screened than those in the bulk simply because there is less material nearby. This effect will be reduced or compensated by the presence of the Pb overlayer. Thus, final-state screening effects in the present case are likely to be much less compared to the model calculation of Karlsson, Nyqvist, and Kanski. The Pb overlayer simply provides a more bulklike environment for the Si surface atoms, both in the initial state and in the final state.

As argued by Le Lay and Hricovini,[3] there is also the possibility that the interface structure changes as a thick Pb overlayer is built up on top of the interface. Since there are no data as yet for the interface structure studied in the electrical measurements of Heslinga *et al.*,[4] this point will require further work for clarification. In addition, the electronic structure of the metal overlayer evolves as a function of thickness, which can also affect the electronic transport across the interface.[26,27]

From the above discussion, it is clear that photoemission determination of Schottky-barrier heights for monolayer-thick overlayers can be inaccurate (~ 0.2-eV errors) in predicting the electrical performance of device configurations, although it has been demonstrated to be quite useful for a survey of the general chemical trend for various systems.[28] The systems studied here are not really metal-semiconductor interfaces. To be complete with the discussion, it should also be pointed out that different electrical measurements do not necessarily yield the same barrier height. For example, the current-voltage measurement of Heslinga *et al.* for the RT phase yielded a barrier height of 0.62 ± 0.02 eV which is different from the 0.70 ± 0.02 eV determined by the capacitance-voltage measurement. This difference is not understood yet. The Schottky-barrier issue has been a subject of intense debate for many years; the systems studied here serve to illustrate some of the problems.

D. Desorption and the β and γ phases

Annealing the α phase to temperatures above the Pb melting point ($>340°$ C) in the desorption regime leads to a $(\sqrt{3}\times\sqrt{3})R30°$ pattern with very sharp $\frac{1}{3}$-order diffraction spots as well as low background and well-defined Kikuchi lines. The general quality of the HEED pattern is comparable to ones obtained for the clean Si(111)-(7×7) surface. The $\frac{1}{3}$-order spots appear first at about 0.9-ML Pb coverage, and gradually sharpen as more Pb is desorbed.

We have studied the evolution of the Si $2p$ and Pb $5d$ cores as a function of annealing time for desorption at 420 and 480 °C. To acquire coverage information versus annealing time, we utilized our RT adsorption data (shown in Fig. 1), which gives the absolute Pb $5d$ intensity and the I(Pb $5d$)/I(Si $2p$) intensity ratio as a function of Pb coverage. The results for 420 and 480 °C desorption are shown in Figs. 5(a) and 5(b), respectively. Each of these curves shows three linear regimes, with clearly defined break points at about $\frac{1}{3}$- and $\frac{1}{6}$- ML Pb coverage. These results are in good agreement with ones obtained recently using Rutherford backscattering spectroscopy,[15] except that this work also noted a break at 0.8 ML. We will denote these phases, whose coverages are $\frac{1}{3}$ and $\frac{1}{6}$ ML, as the β and γ phases, respectively.

The evolution of the Si $2p$ core, during desorption at 420 °C, is shown in Fig. 6. The line shape evolves gradually from a single spin-orbit split doublet for the initial α phase to at least three doublets, which modulate in relative intensity as more Pb is desorbed. At $\frac{1}{3}$-ML Pb coverage (the β phase), the Si $2p$ core may be resolved into three doublet peaks, as shown in Fig. 7. The fitting parameters, together with those for the clean Si(111)-(7×7)

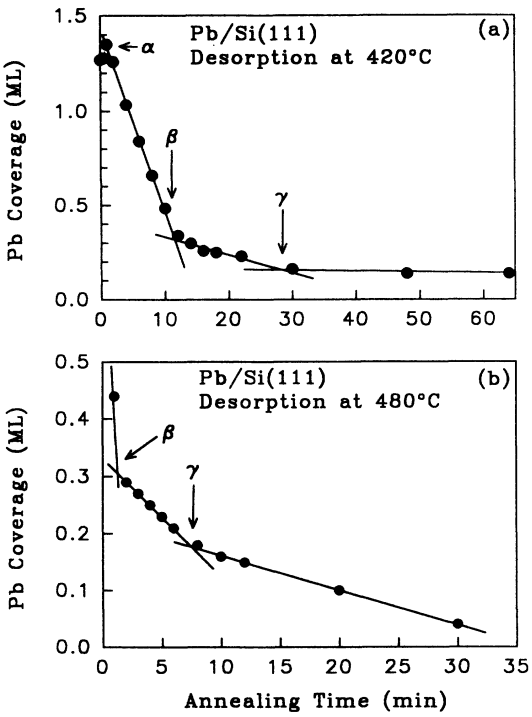

FIG. 5. Isothermal desorption spectra obtained for (a) 420 °C anneals and (c) 480 °C anneals. The coverage of Pb in ML is plotted vs total annealing time in minutes. The coverage is deduced from core-level intensities of photoemission acquired at room temperature. The desorption curves show three linear regimes with two clearly defined break points at $\frac{1}{3}$ and $\frac{1}{6}$ ML. These break points correspond to the β and γ phases, respectively.

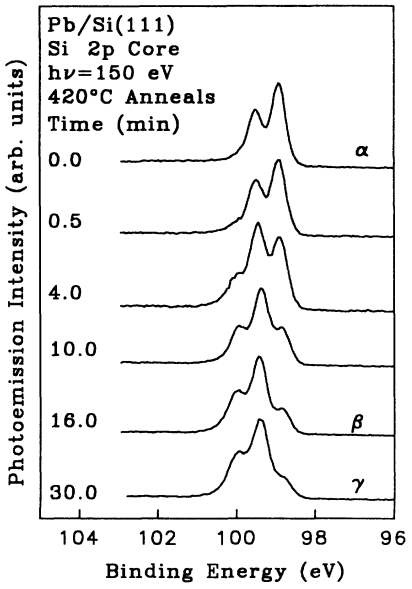

FIG. 6. Selected Si $2p$ spectra obtained after annealing at 420 °C. Total annealing time is shown in minutes to the left of each spectrum. The bottom two spectra correspond to the β and γ phases as indicated.

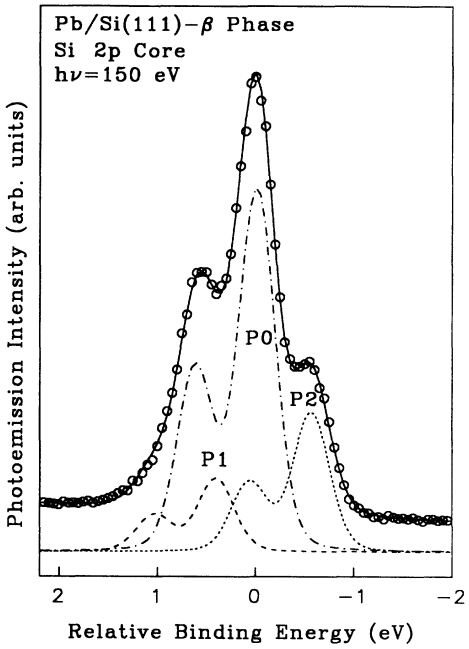

FIG. 7. A Si $2p$ spectrum for the β phase, obtained using 150-eV photons. Circles represent the data whereas the solid curve is the least-squares fit. The decomposition of the spectrum into three components $P0$, $P1$, and $P2$ are indicated by the various curves. The binding energy scale is referred to the bulk $2p_{3/2}$ line. The fitting parameters are summarized in Table I.

spectrum shown in Fig. 2, are summarized in Table I. Based on a comparison with a bulk-sensitive Si $2p$ spectrum obtained using 110-eV photons (not shown), we concluded that the $P1$ and $P2$ components are associated with surface emission, whereas $P0$ represents bulk emission. The $P1$ component is shifted by 0.4 eV to higher binding energy with respect to the bulk component $P0$, and shows a nearly constant emission intensity versus Pb coverage in the $\frac{1}{3}$- to $\frac{1}{6}$-ML range, with respect to the bulk intensity $P0$. The $P2$ component is shifted by 0.57 eV to lower binding energy, and shows an emission inten-

TABLE I. Fitting parameters for the surface-sensitive Si $2p$ core-level line shape for clean Si(111)-(7×7) and the β phase. All energies are in eV. The Lorentzian and Gaussian widths refer to the full width at half maximum. Binding-energy shifts are referred to the bulk components $S0$ and $P0$ of the clean Si(111)-(7×7) and the β phase, respectively. The bottom two lines show the intensity ratios.

	Clean (7×7)	β phase
Spin-orbit splitting	0.610	0.610
Branching ratio	0.500	0.500
Gaussian width	0.205	0.170
Lorentzian width	0.070	0.070
$S1$ ($P1$) shift	−0.405	−0.403
$S2$ ($P2$) shift	0.750	0.570
$I(S1\ (P1))/I(S0\ (P0))$	0.296	0.220
$I(S2\ (P2))/I(S0\ (P0))$	0.105	0.395

sity which is strongly correlated to the Pb coverage. At $\frac{1}{3}$-ML Pb coverage, the magnitude of the $I(P2)/I(P0)$ intensity ratio is 0.40, which is about four times that of the $I(S2)/I(S0)$ ratio for the clean Si(111)-(7×7) surface (see Table I and Fig. 2). As shown in previous studies, the $S2$ component for the clean surface is associated with the Si adatoms of the (7×7) reconstruction, which have a coverage of $\frac{12}{49}$ ML.[21–23] Thus, the $P2$ component for the β phase corresponds to emission from 1 ML of Si atoms.

As discussed above, the best model for the α phase is a close-packed Pb overlayer (1.3 ML) on a bulk-truncated Si substrate. The β phase is obtained from this α phase by desorbing 1-ML Pb from the surface; its structure is therefore likely to be $\frac{1}{3}$ ML of Pb decorating a bulk-truncated Si(111). The $P2$ component, having an intensity corresponding to 1 ML of Si, can be assigned to atoms in the top half of the first Si bilayer closest to the Pb adlayer. The $P1$ component, whose intensity is less than the $P2$ component, most probably represents emission from the other half of the first bilayer. Given that the Pb coverage at this point is $\frac{1}{3}$ ML, we obtain a Pb to Si bonding coordination number of 3 within this model. The easiest interpretation of these results, in light of the $(\sqrt{3}\times\sqrt{3})R30°$ periodicity of the reconstruction, is that each Pb atom is bonded to three Si surface atoms in either a T_4 or H_3 geometry. The T_4 geometry is more likely based on a theoretical study.[29]

In the above model for the β phase, all of the Si dangling bonds are replaced by Si—Pb chemisorption bonds. Since Pb and Si are in the same column of the Periodic Table, one might expect that there should be very little chemical shift for Si induced by bonding to Pb.[25] However, a significant chemical shift is observed for the Si surface atoms. We believe that this is due to the threefold coordination of the Pb, which is not compatible with its chemical valence. As a result, a partial charge transfer (electronic rearrangement) occurs between Si and Pb, which induces such chemical shifts.

The Si $2p$ core level obtained for the γ phase at $\frac{1}{6}$-ML Pb coverage looks fairly similar to that for the β phase at $\frac{1}{3}$-ML Pb coverage; the comparison is shown in Fig. 8. The main difference is that the intensity of the peak at the lower binding energy side (the $P2$ peak for the β phase) is reduced. The reduction is about 30% from a three-component fit. A recent STM study has shown evidence that the γ phase consists of a mixture of $\frac{1}{6}$-ML Pb adatoms and $\frac{1}{6}$-ML Si adatoms arranged in a $(\sqrt{3}\times\sqrt{3})R30°$ pattern on top of a bulk-truncated Si(111). In other words, the γ phase is obtained from the β phase by replacing half of the Pb adatoms on the surface by Si adatoms. With this replacement, we expect that the intensity of the $P2$ component for the β phase (see Fig. 7) will be reduced by 50%, because this component arises from a Pb-induced chemical shift. The $\frac{1}{6}$-ML Si adatoms now on the γ surface should exhibit a core-level energy shift of about −0.75 eV relative to the bulk [−0.75 eV is the shift of the $S2$ (adatom) component for clean Si(111)-(7×7)]. This shift is very close to the Pb-induced $P2$ chemical shift of −0.57 eV, and we do not expect to be able to resolve these separate components reliably based on a multiple-component fit. If we ignore this slight energy difference, the intensity of the peak on the low-binding-energy side should change from 1 ML for the β phase to $(\frac{1}{2}+\frac{1}{6}=\frac{2}{3})$ ML for the γ phase, and this predicted one-third intensity reduction of the $P2$ peak is consistent with our finding. With further annealing at high temperatures of the γ phase, the Si core-level line shape eventually becomes that of clean Si(111)-(7×7) when all of the Pb is desorbed.

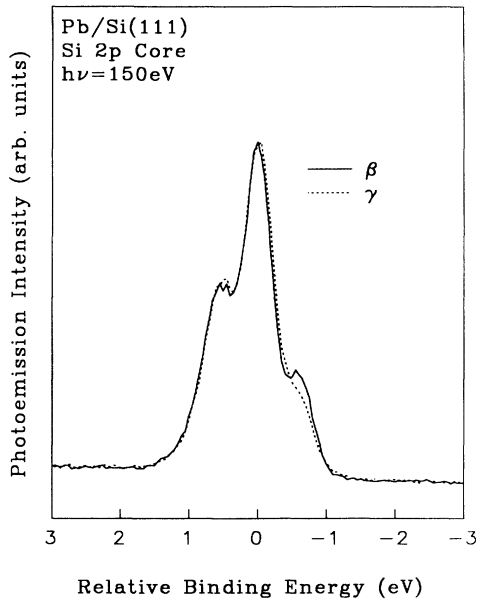

FIG. 8. A comparison of the Si $2p$ spectra for the β and γ phases obtained during the 480 °C annealing sequence. The two spectra are normalized to have the same area.

E. Valence-band spectra

The valence-band spectra for clean Si(111)-(7×7), the RT phase, and the α, β, and γ phases are shown in Fig. 9. The clean Si(111)-(7×7) surface exhibits three surface states as indicated by arrows in the figure.[21,29,30] Upon RT adsorption these states are quickly quenched, resulting in a valence band with a rather large density of states at ~1.2 eV below the Fermi level E_F. Annealing moves the maximum density of states to about 0.9 eV below the Fermi level for the α phase. In our angle-integrated geometry we do not clearly discern any surface states for the α phase, but in other work,[10,11] using a normal emission and angle-resolving geometry, a nondispersing feature at about 0.9 eV below E_F is prominent. This surface state (probably resonance) persists even at 375 °C (i.e., above the Pb melting point at 340 °C), when the periodicity is (1×1). For this reason it has been speculated that the reversible phase transition mentioned earlier is not associated with a two-dimensional melting transition, but rather an order-disorder one.[10,11]

For the β phase, two well-defined surface states at approximately 0.6 and 1.4 eV below E_F are observed, as indicated by the arrows in Fig. 9. Similar surface states

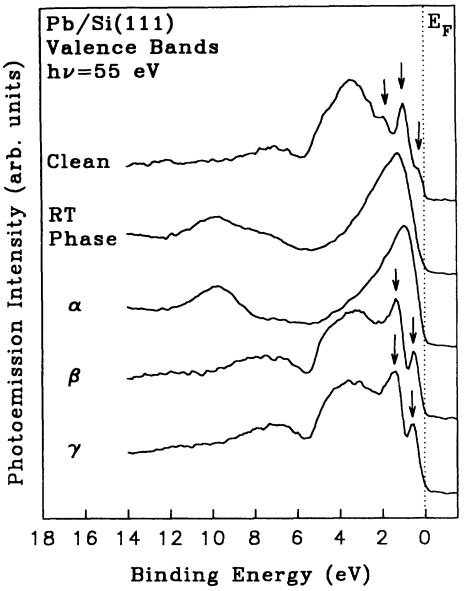

FIG. 9. Valence-band spectra obtained for the clean Si(111) (7×7) surface, the RT phase, and the α, β, and γ phases. The last two spectra were obtained after annealing at 420 °C and the corresponding Si 2p cores are shown in Fig. 6. The arrows indicate surface-state positions.

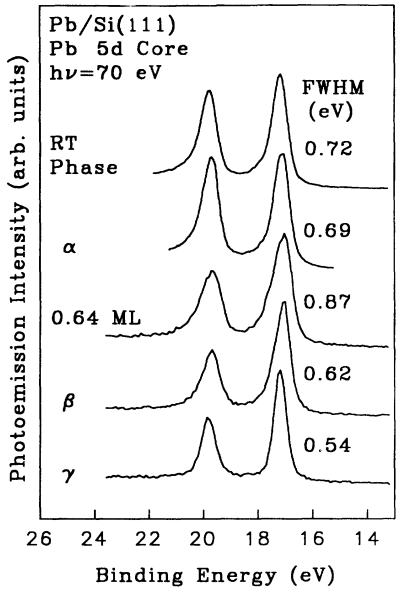

FIG. 10. Pb 5d spectra, acquired using 70-eV photons for the RT phase, the α phase, a sample with 0.64-ML Pb coverage after desorbing some Pb from the α phase, and the β and γ phases. The full width at half maximum (FWHM) of the Pb $5d_{5/2}$ component is recorded to the right of each spectrum.

have been observed for the $(\sqrt{3}\times\sqrt{3})R30°$ surface of Al-adsorbed Si(111).[31] Based on this information and our discussions of the core-level results and structural model for the β phase, we assign the origins of these surface states to Pb adatoms bonded in a T_4 geometry. Following the theoretical study by Northrup,[29] who studied a $(\sqrt{3}\times\sqrt{3})R30°$ arrangement of Si T_4 adatoms on a bulk-truncated Si(111) surface, the surface state at 0.6 eV below E_F is derived from substrate dangling-bond states coupled to Pb adatom p_z orbitals, and the surface state at 1.4 eV below E_F arises from substrate dangling bonds coupled to Pb adatom p_x and p_y orbitals. This assignment is in agreement with STM results.[15]

By replacing half of the Pb adatoms of the β phase by Si adatoms, the γ phase is formed, and the valence-band spectra remain essentially unchanged (see Fig. 9). This is in agreement with the above interpretation since all of the T_4 sites are still saturated, either by Pb or by Si. The results of Al on Si and Si on Si mentioned above show that the binding energies of these surface states are not very sensitive to the atomic identities of the species occupying the T_4 sites.

Of all of the spectra in Fig 9, only the one for Si(111)-(7×7) shows a clear metallic Fermi edge. The other spectra do show a tail reaching the Fermi level, indicating that these surfaces are weakly metallic, as mentioned earlier.

F. Pb 5*d* core

Shown in Fig. 10 are Pb 5d core levels for the RT phase, the α phase, a surface covered with 0.64-ML Pb obtained by desorbing Pb from the α phase, and the β and γ phases. For the RT growth, the Pb 5d core shows an initial full width at half maximum (FWHM) of 0.80 eV at 0.1 ML, which gradually narrows to 0.72 eV at 1.3-ML coverage. Upon annealing at 240 °C to form the α phase, the Pb 5d core narrows slightly to 0.69 eV. Further changes are observed upon annealing at temperatures in excess of 400 °C, to form the β and γ phases. As Pb is desorbed from the surface, its FWHM increases to a maximum of 0.87 eV at ~0.6 ML, after which it decreases rapidly to 0.62 eV at $\frac{1}{3}$ ML and further to 0.54 eV at $\frac{1}{6}$-ML Pb coverage and below. The varying width of the Pb 5d core is likely a result of multiple unresolved components in the spectrum due to the presence of inequivalent sites and/or due to the varying degrees of ordering of these surfaces. The apparent position of the Pb peak shows a very slight shift to higher binding energy at $\frac{1}{3}$ and $\frac{1}{6}$ ML as compared to 1.3-ML Pb coverage. Also noted is a change in the branching ratio. It is 0.83 for the RT phase and 0.89 for the α phase. With high-temperature annealing and the gradual removal of Pb, the branching ratio decreases to 0.55 at $\frac{1}{3}$-ML Pb coverage and below. These values are compared with the bulk value of 0.72 [obtained from a 100-ML Pb deposit onto a Si(111) substrate held at 250 °C] and the statistical value of $\frac{2}{3}=0.67$. A similar dependence of branching ratio on adsorbate coverage has previously been observed for the Cs/W(100) system.[32] This coverage dependence of the branching ratio indicates a solid-state effect as opposed to a purely atomic mechanism. The Pb 5d doublet could possess bandlike character for the higher coverage phases; we note that this was indeed found for the Cs 5p peaks.[32] The Pb 5d doublet is not quite as shallow as the Cs 5p levels, however (~18 eV as compared to ~12 eV).

IV. SUMMARY

High-resolution photoemission spectroscopy utilizing synchrotron radiation and HEED have been employed to probe the RT growth and isothermal desorption of Pb on Si(111) surfaces. We have confirmed the SK growth mode for this system and found that the first adlayer is completed at 1.3 ML. This is an epitaxial (7×7) phase consisting of a close-packed Pb overlayer on an unrelaxed, partially faulted Si substrate. After annealing to above about 200 °C, the close-packed Pb overlayer rotates by 30° and forms an incommensurate overlayer with an approximate $(\sqrt{3}\times\sqrt{3})R30°$ structure over a bulk-truncated Si(111). The anneal appears to remove the stacking fault in the Si(111) substrate. This is the α phase. With increasing substrate temperature, this α phase undergoes a reversible phase transition at 280 °C to a (1×1), and if the temperature is further increased to over 340 °C, significant Pb desorption begins. After some Pb is removed from the surface, two distinct $(\sqrt{3}\times\sqrt{3})R30°$ phases, the β and γ phases, are found. The β phase consists of a $\frac{1}{3}$-ML Pb overlayer bonded in T_4 sites on a bulk-truncated Si(111). The γ phase is obtained from the β phase by replacing one-half of the Pb adatoms by Si adatoms. These structural models are supported by our detailed core-level and surface-state measurements.

The band bending induced by the adsorbed Pb has been studied. We determined n-type Schottky barrier heights of 0.89 and 1.09 eV for the RT and α phases, respectively. These barrier heights are each larger by about 0.18 eV than the corresponding values determined from capacitance-voltage measurements for the same two reconstructed surfaces overcoated with a thick Pb overlayer. However, the barrier-height difference between the two phases is the same for the two different measuring techniques; this is consistent with the expectation that the barrier-height difference is a local effect specific to the interface structural difference. The discrepancy between photoemission and electrical measurements for each reconstruction may be simply related to the difference in Pb overlayer thickness; effects such as core-hole screening, subsurface shifts, and quantum size effects associated with the monolayer configuration can cause a difference. Furthermore, structural changes which occur in the first Pb layer due to the presence of a thick Pb film can also cause the barrier height to change. Since the structure of these buried interfaces is unknown, this point will require further investigation. This work shows that photoemission prediction of electrical performance of device configurations suffers inaccuracies on the order of 0.2 eV.

ACKNOWLEDGMENTS

This material is based upon work supported by the U.S. Department of Energy (Division of Materials Sciences, Office of Basic Energy Sciences), under Grant No. DEFG02-91ER45439. Acknowledgment is also made to the Donors of the Petroleum Research Fund, administered by the American Chemical Society, and to the U.S. National Science Foundation (Grant No. DMR-89-19056) for partial financial support. We acknowledge the use of central facilities of the Materials Research Laboratory of the University of Illinois, which is supported by the U.S. Department of Energy (Division of Material Sciences, Office of Basic Energy Sciences), under Grant No. DEFG02-91ER45439, and the U.S. National Science Foundation under Grant No. DMR-89-20538. The Synchrotron Radiation Center of the University of Wisconsin—Madison is supported by the U.S. National Science Foundation.

[1]G. Le Lay, K. Hricovini, and J. E. Bonnet, Appl. Surf. Sci. **41/42**, 25 (1989).
[2]D. R. Heslinga, H. H. Weitering, D. P. van der Werf, T. M. Kalpwijk, and T. Hibma, Phys. Rev. Lett. **64**, 1589 (1990).
[3]G. Le Lay and K. Hricovini, Phys. Rev. Lett. **6**, 807 (1990).
[4]H. H. Weitering, D. R. Heslinga, T. Hibma, and T. M. Klapwijk, Phys. Rev. Lett. **6**, 808 (1990).
[5]K. Karlsson, O. Nyqvist, and J. Kanski, Phys. Rev. Lett. **67**, 236 (1991).
[6]P. J. Estrup and J. Morrison, Surf. Sci. **2**, 465 (1964).
[7]M. Saitoh, K. Oura, K. Asano, F. Shoji, and T. Hanawa, Surf. Sci. **154**, 394 (1985).
[8]H. Yaguchi, S. Baba, and A. Kinbara, Appl. Surf. Sci. **33/34**, 75 (1988).
[9]G. Le Lay, J. Peretti, M. Hanbücken, and W. S. Yang, Surf. Sci. **204**, 57 (1988).
[10]G. Le Lay, K. Hricovini, and J. E. Bonnet, Colloq. Phys. **50**, 210 (1988).
[11]G. Le Lay and M. Abraham, in *Kinetics of Ordering and Growth at Surfaces* (Plenum, New York, 1990), p. 209.
[12]G. Quental, M. Gauch, and A. Degiovanni, Surf. Sci. **193**, 212 (1988).
[13]G. Quental, M. Gauch, A. Degiovanni, W. S. Yang, J. Peretti, M. Hanbücken, and G. Le Lay, Phys. Sci. **38**, 123 (1988).
[14]F. Grey, R. Feidenhans'l, M. Nielsen, and R. L. Johnson, Colloq. Phys. C **7**, 181 (1989); R. Feidendans'l, F. Grey, M. Nielson, and R. L. Johnson, in *Kinetic Ordering and Growth at Surfaces* (Plenum, New York, 1990), p. 189.
[15]E. Ganz, F. Xiong, Ing-Shouh Hwang, and J. Golovchenko, Phys. Rev. B **43**, 7316 (1991).
[16]T. N. Doust and S. P. Tear, Surf. Sci. **251/252**, 568 (1991).
[17]T. Ichikawa, Solid State Commun. **46**, 827 (1983); **49**, 59 (1984).
[18]K. Hricovini, G. Le Lay, A. Kahn, A. Taleb-Ibrahimi, J. E. Bonnet, L. Lassabatére, and M. Dumas, Surf. Sci. **251/252**, 424 (1991).
[19]H. H. Weitering, T. Hibma, D. R. Heslinga, and T. M. Klapwijk, Surf. Sci. **251/252**, 616 (1991).
[20]D. H. Rich, T. Miller, and T.-C. Chiang, Phys. Rev. Lett. **60**, 357 (1988).
[21]A. Samsavar, T. Miller, and T.-C. Chiang, Phys. Rev. B **42**, 9245 (1990).
[22]D. H. Rich, T. Miller, and T.-C. Chiang, Phys. Rev. B **37**, 3124 (1988).

[23]J. A. Carlisle, T. Miller, and T.-C. Chiang, Phys. Rev. B **45**, 3811 (1992).

[24]F. J. Himpsel, F. R. McFeely, J. F. Morar, A. Taleb-Ibrahimi, and J. A. Yarmoff, in *Photoemission and Adsorption Spectroscopy of Solids and Interfaces with Synchrotron Radiation,* Proceedings of the International School of Physics "'Enrico Fermi," Course CVIII, Varenna, Italy, 1988 [Nuovo Cimento (to be published)].

[25]T.-C. Chiang, CRC Crit. Rev. Solid State Mater. Sci. **14**, 269 (1988).

[26]A. L. Wachs, A. P. Shapiro, T. C. Hsieh, and T.-C. Chiang, Phys. Rev. B **33**, 1460 (1988).

[27]M. A. Mueller, A. Samsavar, T. Miller, and T.-C. Chiang, Phys. Rev. B **40**, 5845 (1989).

[28]G. Margaritondo, Phys. Today **41** (4), 66 (1988).

[29]John E. Northrup, Phys. Rev. Lett. **57**, 154 (1986).

[30]R. J. Hamers, R. M. Tromp, and J. E. Demuth, Phys. Rev. Lett. **55**, 1303 (1985).

[31]R. I. G. Ubrberg, G. V. Hansson, J. M. Nicholls, and P. E. S. Persson, Phys. Rev. B **31**, 3805 (1985).

[32]N. V. Smith, P. K. Larsen, and S. Chiang, Phys. Rev. B **16**, 2699 (1977).